Development of Force Control and Proprioception on a Closed Chain 5-Segment Leg

Gavin Foster[1*]*, Amir* Patel[1,2,], and *Stacey* Shield[1]

[1]African Robotics Unit, Department of Electrical Engineering, University of Cape Town, South Africa
[2]Department of Computer Science, University College London, United Kingdom

Abstract. In this paper we demonstrate a simple and equipment-light manner of tuning the actuation and proprioception of Spring-Loaded Inverted Pendulum (SLIP) control for a 5-segment monoped. We show that with simple calibration tests, one can greatly improve the accuracy of force commands as well as motor proprioception, reducing mean percentage error for actuation from 19.7% to 6.4 %, and reducing vertical force proprioception accuracy from 38.0% to 4.1%. This low-level force accuracy allows for much greater accuracy in control schemes utilizing vertical force control. It was shown however that the same methods could not be utilized successfully for horizontal forces.

1 Introduction

Control of robotic systems is greatly benefitted by the accuracy of commands (i.e. how close the output of the actuator is to the commanded output) undertaken by the robot and the accuracy of sensors to feed back the result of that command. Specifically, in the world of legged robotics, good locomotion relies on accuracy in both these regards.

A widely used approach for the modelling and control of legs, of both robots and creatures alike, is the template of a Spring Loaded Inverted Pendulum (SLIP) [1]. Roboticists can use this to model a leg as a more universal and geometrically simpler system to create more universal control strategies for bipedal robots, for example in [2].

Using this template, we can abstract a given leg geometry into a force actuator acting from body to foot (or point of contact), however this abstraction is likely to add inaccuracies due to the difference in both actuation and feedback (proprioception). Methods of minimizing these inaccuracies are primarily found in the design of the robotic legs [3, 4], rather than in their control. Despite the design for maximum force transparency, both in actuation and in feedback, there is room for improvement, and a more accurate actuator and sensor pair allows for more accurate control of the system. This is reinforced by our study of animal proprioception [5].

---

* Corresponding author: fstgav002@myuct.ac.za

In this paper, we propose a simple and accessible way to calibrate force actuation and foot force proprioception on a legged robot using a basic experimental setup utilizing only a 5-segment monoped and a force sensor. This method is proposed as a more cost-effective way to calibrate leg (and hence motor) dynamics and parameters compared to methods involving torque sensors.

2 Methodology

This section discusses the methods used to create and validate the proposed method of tuning proprioception and actuation.

2.1 Experimental overview

The experimental calibration involves using a SLIP template based control scheme with fixed parameters on a robot's leg. The leg is then put on a force plate or force transducer, and a force is applied by hand to the robot. The reaction force that the robot reads via motor current as well as the force experienced by the reference (or ground truth) force plate are then measured.

2.2 Equipment

The experimental equipment utilized are the African Robotics Unit (ARU)'s planar monoped robot "Half-leka", and an Axia80-m20 force sensor set up as a force plate. The robot is attached to a planarizing boom, simplifying the system to two dimensions. Half-leka is a basic robot monoped that consists of two T-motor AK10-9 V3.0 brushless DC motors which actuate its 5-segment scissor legs. The robot is a single leg version of the ARU's full biped, Baleka, which is designed for studying rapid manoeuvrability [3, 6]. Both Half-leka and the force plate are controlled and communicated with using a Speedgoat Baseline running MATLAB Simulink code. The experimental setup is shown in Figure 1 below.
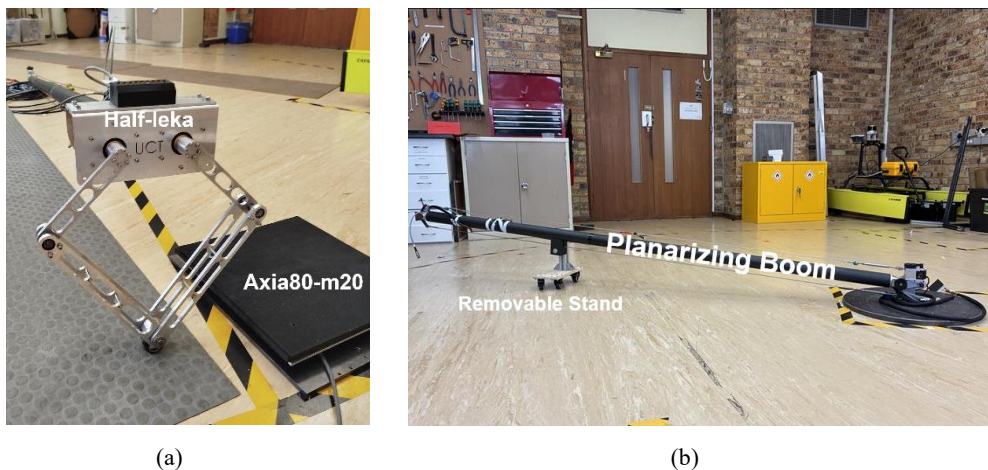

<div align="center">(a)   (b)</div>

Fig. 1. (left) Half-leka on its planarizing boom next to an Axia80-m20 set up as a force plate. (right) Sideways view of the planarizing boom sitting on a removable rolling stand (robot not mounted).

The data gathered for these experiments included motor angles, motor velocities, motor current readings, and the 6-axis force/torque readings from the Axia80-m20, all of which were captured at 1 kHz.

2.3 Theory and Control
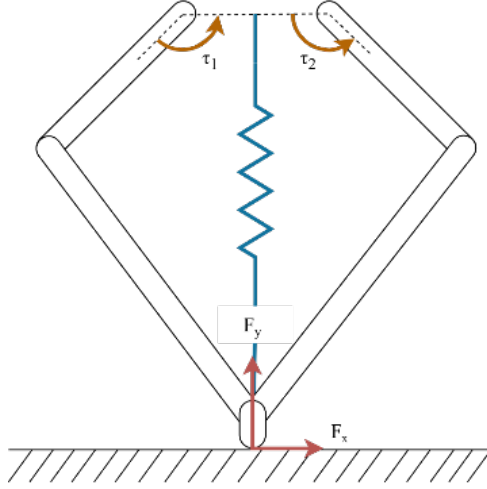
A diagram of the leg is shown in Figure 2 below.

Fig. 2. Diagram of the 5-segment legs

The robot's legs are controlled via torques τ_1 and τ_2 applied by two motors at the hip. These are used to control the forces at the foot $[F_x \quad F_y]^T$. The fundamentals of the control and proprioception are governed by the following equation [4]:

$$\begin{bmatrix} \tau_1 \\ \tau_2 \end{bmatrix} = \mathbf{J^T}_{xy} \begin{bmatrix} F_x \\ F_y \end{bmatrix} \tag{1}$$

Where $\mathbf{J_{xy}}$ is the leg's Jacobian matrix. This equation is a greatly simplified version of the manipulator equation (neglecting most terms) as shown in [4]. It is utilized in the leg controller in two directions, either to calculate the torque to be applied to the motors to achieve a desired ground reaction force, or to use measured motor current to calculate the ground reaction forces being applied at the foot.

The spring shown in Figure 2 indicates the 'virtual leg', which is the controlled vector between the robot's body and its foot. This is controlled using a SLIP model where the control scheme uses spring and damping constants which govern the movement of the angle and length of the virtual leg by actuating appropriate torques which make the leg behave as if it was a SLIP. The SLIP abstraction utilizes a different Jacobian, as instead of translating between motor torques and x and y forces, it translates between motor torques and r forces and θ torques, which are defined as forces parallel to the virtual leg, and torques rotating about the virtual leg. This Jacobian will be referred to as $\mathbf{J^T}_{r\theta}$.

The torque commands for the SLIP leg are then defined as:

$$\begin{bmatrix} \tau_1 \\ \tau_2 \end{bmatrix} = \mathbf{J^T}_{r\theta} \begin{bmatrix} K_{Pr}(r_d - r) - K_{Dr}(\dot{r}) \\ K_{P\theta}(\theta_d - \theta) - K_{D\theta}(\theta) \end{bmatrix} \tag{2}$$

Where K_{Pr} is the leg spring constant (N/m). r_d is the desired leg (spring) neutral length (m). r is the virtual leg length (m). K_{Dr} is the leg damping constant (Ns/m). $\dot{r}$ is the rate of change in leg length (m/s). $K_{P\theta}$ is the rotational spring constant (N/rad). θ_d is the desired leg

(spring) angle (rad). θ is the virtual leg angle (rad). $K_{D\theta}$ is the leg angle damping constant (Ns/rad). $\dot{\theta}$ is the rate of change in leg angle (rad/s).

Using these parameters the behaviour of the SLIP leg can be dictated.

For the coordinate system, Figure 2 shows the coordinates of the legs as viewed from the sagittal plane towards the boom (i.e. the perspective of Figure 1a), with angles measured counterclockwise from the positive x-axis.

2.4 Experimental method

The experimental setup is to have the robot's foot resting on a force plate, with leg control configured to have a fixed spring constant, and some damping for stability, and to keep itself vertical (virtual leg at -90°). The robot is then pushed onto the force plate by hand to vary the forces created at the foot by the torques generated by the motors. The robot is pushed both downwards and from side to side along its sagittal plane to create both vertical and horizontal forces at the foot. The force plate measures the ground truth data for the forces at the foot, while the robot's motor commands and currents were recorded for the calibration. This routine was repeated several times at different set spring constants (K_{Pr}) of 1000 N/m, 1250 N/m, 1500 N/m, 1750 N/m and 2000 N/m to vary the forces and leg displacement in the data. The other parameters were set as the following as shown in Table 1:

Table 1. Experimental set parameters

Parameter	Value
K_{Dr}	50 Ns/m
$K_{P\theta}$	150 N/rad
$K_{D\theta}$	10 Ns/rad
r_d	0.45 m
θ_d	$-\pi/2$

This data is then analysed for linear fits for calibration coefficients. The experiment was done twice, firstly to calibrate the actuation of the motors such that the force commanded to the leg was better related to the force realized by the leg, and then secondly to validate the actuation calibration as well as gather data to be used for proprioception calibration.

The actuation calibration was quantified by plotting the ground truth torque as measured by the force plate (having been translated via the Jacobian), and the torque commanded to the motors. Both motors were fit on the same set of axes to create a uniform proportionality constant regardless of direction. This plot was then fit to a linear distribution without an offset to find a best fit scaling coefficient for input torque commands.

For proprioception, the direct force plate measurements were compared to the foot force measured by the motors using motor current (and translated via the inverse Jacobian). The horizontal (x) and vertical (y) forces were analysed separately, with linear fits for each of them forming compensation coefficients.

It is worth noting that the experiment was limited to constant contact with the force plate, and so any drops or hops were avoided. While modelling more dynamic motions, especially

impacts, would benefit the experiment, the instantaneous nature of impacts results in artifacts on the force sensor readings that render the readings inaccurate.

3 Data and Analysis

3.1 Actuation fit and calibration

Using the results of the first experiment, the commanded motor torque for both motors was plotted against the realized torque as measured by the force sensor readings which were translated via the Jacobian. This plot is shown in Figure 3 below.
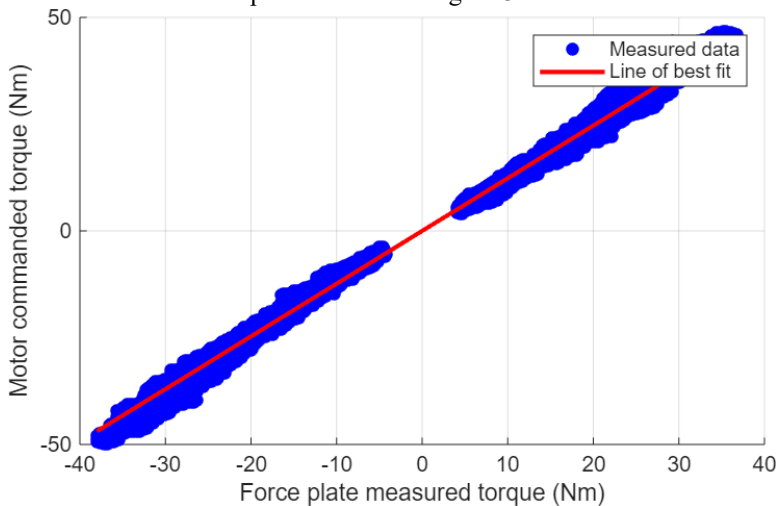

Fig. 3. Scatter plot of force plate measured torque vs motor commanded torque

This was fit linearly, but specifically without a constant offset as opposed to a standard line of best fit including a constant offset. The reason for this is twofold, firstly, this data uses both the left and right motor, and so symmetry between directions is expected, as the motors should have near-identical physical properties, and an offset would result in motor torque being commanded when none should be, which poses a safety and control risk.

The actuation data showed a strong linear fit, with an R^2 value of 0.996 and a gradient of 1.23. This indicates that there is a scaling factor of 1.23 between commanded torque and actuated torque which can then be used to compensate and more correctly create the desired torque.

3.2 Proprioception fit and calibration

Following this, the proprioception was analysed. This was done with vertical and horizontal forces separately. The force measured by the motors, which was done by converting the current measurement via the torque constant and then translating via the inverse Jacobian as in Equation 1, was compared to the force measured by the force sensor. The scatter plot for vertical forces is shown in Figure 4 below.
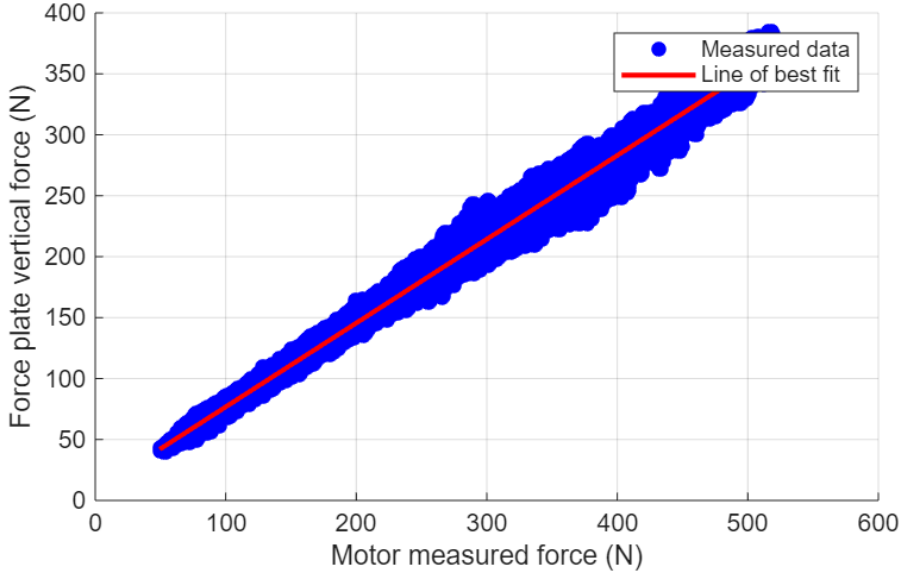

Fig. 4. Scatter plot of force plate vertical force vs motor measured vertical force

As is clearly seen in Figure 4, there is a strong linear fit. This corresponds to an R^2 value of 0.993. The scaling of motor force to force sensor force is given by:

$$y = 0.687x + 8.02 \tag{3}$$

Where x is the motor measured vertical force, and y is the compensated reading vertical force.

This allows us to compensate vertical force measurements by scaling them by Equation 3 to have a more accurate measurement of vertical force.

The horizontal forces however, showed far less promise, as shown in the scatter plot of Figure 5.
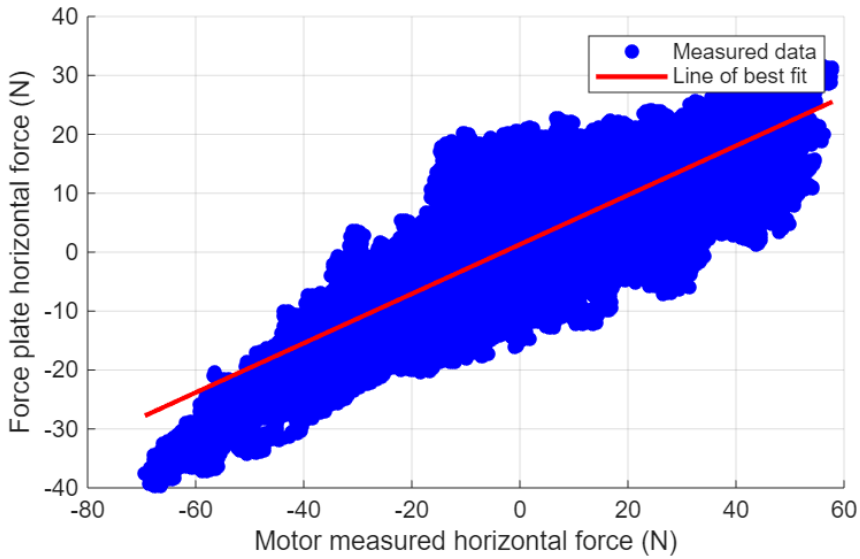
Fig. 5. Scatter plot of force plate horizontal force vs motor measured horizontal force

As can be seen, the horizontal force proprioception has far less potential to be fit, linear or otherwise, and the data is overall very scattered. Unlike the previous two fits, this set of data shows a weak linear fit, with an R^2 value of 0.57. The overall shape indicates that compensation for these measurements is extremely unlikely to yield any meaningful results, and as such, compensating for horizontal force measurements was deemed infeasible.

3.3 Validation and Results

The compensation for actuation and vertical proprioception were validated with additional validation test data.

For actuation, this was done by comparing the mean percent error between the data gathered without compensation to the mean percent error for the data gathered while compensated. This resulted in the error between commanded torque and realized torque decreasing in mean percent error from 19.7% to 6.4%.

For proprioception, the compensation can be measured within the same dataset, rather than with two different tests, as unlike actuation, proprioception does not impact the test itself. When comparing the vertical proprioception measurements before and after compensating using Equation 2, the mean percent error of vertical force measured via proprioception compared to force plate data went from 38.0% when uncompensated, to 4.1% with compensation.

Figures 6 & 7 below show samples of both uncalibrated and calibrated results for vertical forces, demonstrating the improvement in accuracy between commanded force, proprioception force, and the ground truth from the force plate. Samples are shown as the full data used for validation was 200 s in duration, hence a random sample provides more readable visual representation of results.
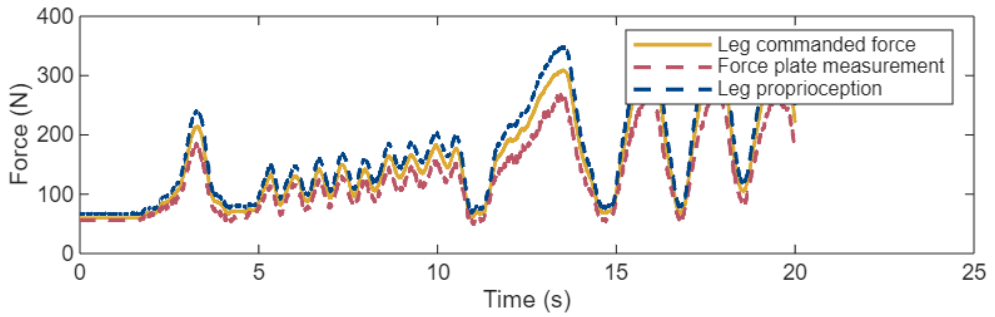
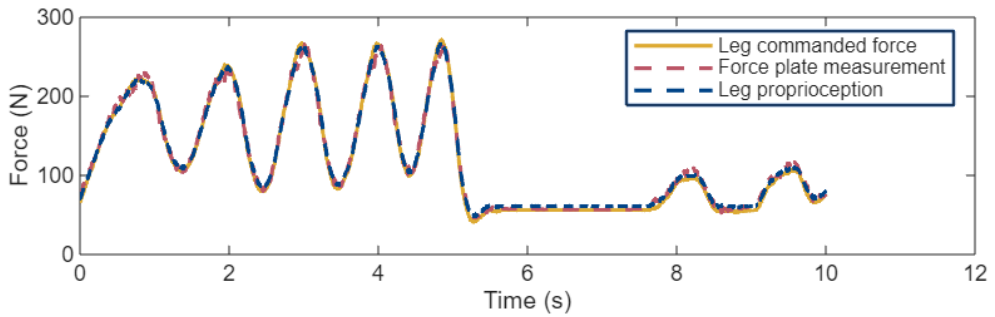**Fig. 6.** Sample of uncalibrated experiment data showing vertical forces

Fig. 7. Sample of calibrated experiment data showing vertical forces

4 Discussion and Conclusion

As is most clearly shown in Figures 6 & 7, the compensation of both actuation and vertical proprioception using linear fits for calibration coefficients results in significant accuracy improvements for force transparency, having reduced the actuation mean percent error from 19.7% to 6.4%, and the proprioception error from 38.0% to 4.1%.

These two results will be a great benefit in upstream control, as the lower-level control and sensing can be relied on more heavily. Having a built-in (via the motor drivers) way to measure vertical forces at the foot with 4.1% accuracy eliminates the need for additional force or pressure sensors at the foot for tasks requiring a rough estimate of ground reaction forces. Additionally, reducing the actuation error results in more modellable behaviour of the robot, and upstream control systems can expect better performance of the commands they give to the force actuation of the leg.

The result for horizontal force proprioception, however, is shown to provide no value. A lack of sensing of horizontal forces could hinder control, especially with respect to foot slippage or rapid horizontal acceleration. The lack of correlation for the forces shown in Figure 5. demonstrates a flaw in the experiment at low force magnitudes. This is likely due to the limitations of current measurement in motors, combined with the geometry of the extended 5-segment leg not being as transparent in terms of horizontal forces at the foot.

These results are limited to constant foot contact with the ground (or force plate), and so future investigation may be warranted in the direction of adding drops and hops to the tests, however force plates are noted for artifacts in high impact loading environments, which would pollute the ground truth data used.

In summary, it is found that the proposed method greatly enhances accuracy of both the actuation and sensing of vertical forces of robotic legs with minimal infrastructure

requirements to do the required testing. However the results of the tuning in the horizontal direction show the limitations of the proposed methods for smaller forces.

References

1. R. J. Full and D. E. Koditschek, Templates and anchors: neuromechanical hypotheses of legged locomotion on land, Journal of Experimental Biology, vol. 202, no. 23, pp. 3325–3332, Dec. 1999, doi: [10.1242/jeb.202.23.3325](10.1242/jeb.202.23.3325).

2. B. Dadashzadeh, H. R. Vejdani, and J. Hurst, From template to anchor: A novel control strategy for spring-mass running of bipedal robots, in 2014 IEEE/RSJ International Conference on Intelligent Robots and Systems, Chicago, IL, USA: IEEE, Sep. 2014, pp. 2566–2571. doi: 10.1109/IROS.2014.6942912.

3. Blom, A. (2019). Design of a bipedal robot for rapid acceleration and braking manoeuvres (Master's thesis). University of Cape Town, Cape Town, South Africa.

4. S. Seok, A. Wang, D. Otten, and S. Kim, Actuator design for high force proprioceptive control in fast legged locomotion, in 2012 IEEE/RSJ International Conference on Intelligent Robots and Systems, Vilamoura-Algarve, Portugal: IEEE, Oct. 2012, pp. 1970–1975. doi: 10.1109/IROS.2012.6386252.

5. C. J. Dallmann, P. Karashchuk, B. W. Brunton, and J. C. Tuthill, A leg to stand on: computational models of proprioception, Current Opinion in Physiology, vol. 22, p. 100426, Aug. 2021, doi: 10.1016/j.cophys.2021.03.001.

6. C. Fisher, A. Blom, and A. Patel, Baleka: A Bipedal Robot for Studying Rapid Maneuverability, Frontiers in mechanical engineering, vol. 6, 2020, doi: 10.3389/fmech.2020.00054.